Q-space Simulations on Mouse Spinal Cord White Matter Tract Histologic Images

H. H. Ong[1], P. K. Saha[1], E. D. Schwartz[1], F. W. Wehrli[1]

[1]Laboratory for Structural NMR Imaging, Department of Radiology, University of Pennsylvania, Philadelphia, Pennsylvania, United States

Introduction

Q-space imaging is a method for indirect assessment of porous material microstructure, yielding measures of pore size at micrometer resolution[1]. The Fourier Transform of the q-space echo attenuation (propagator, Pg), is a molecular displacement probability density function. Therefore, the Pg full-width-at-half-maximum (FWHM) should correlate with the scale of the restrictions – the pore diameter. Previous work has applied q-space imaging to biological structures such as spinal cord (SP) white matter (WM) tracts[2,3]. However, these experiments are complicated by the presence of both extra-cellular (ECF) and intra-cellular (ICF) signal (e.g. water) and the exchange of spins between these compartments, the consequences of which are poorly understood. In this work, we investigate these questions by performing q-space simulations on histologic images of mouse cervical SP WM tracts (cuneatus, gracilis, and rubrospinal tract (RST)), which have characteristically different mean axon sizes, using a diffusion simulation program developed previously[4]. By systematically varying parameters such as membrane/myelin permeability and ECF/ICF T_2 values, we found that presence of ECF and ICF signal and exchange between both compartments to have little or no effect on the Pg FWHM. The Pg FWHMs invariably correlated with the mean axon diameters calculated from the histologic images.

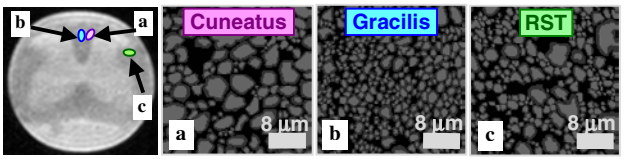

Fig. 1 Stimulated-echo image (left) of a mouse cervical SP indicating anatomic locations of cuneatus (a), gracilis (b) and RST (c) tracts along with their segmented histologic images.

Methods

A SP was dissected from an 8-10 month-old female C57 BL/6 perfusion-fixated mouse. After a myelin stain (toluidine blue), optical microscopic images were obtained for cuneatus, gracilis, and RST regions. The images were then manually segmented into ECF, ICF and myelin regions (Fig.1), and mean axon diameters calculated by equating the ICF area of each axon to a circle. Final images were 128×128 with a pixel size of $0.25\times0.25\mu m^2$. The simulation program is based on a 2-D finite-difference diffusion model and executed a pulsed-gradient spin-echo sequence. It was run on a Dell Precision 670 (dual Xeon 3.6GHz, 4GB). Simulation parameters were: ECF/ICF/myelin diffusion coefficient = $1.65/1.12/1.12\mu m^2/ms$, ECF/ICF/myelin T_2=78/300/19*ms*, zero axon membrane/myelin permeability, TR=1s, TE/Δ/δ=105/15/5*ms*, and diffusion gradients were applied in 64 increments of q (q_{max}=1.34 μm^{-1}). The diffusion coefficient and T_2 values were chosen as in refs[5,6]. Q-space was zero-filled to 128 q-values and Fourier transformed to produce the Pg (resolution $0.75\mu m$ before zero-filling) and FWHM was computed. There is uncertainty in the literature on ECF/ICF T_2 values, so a range of values was chosen. Due to the long TE and ICF T_2, the above parameters lead to ICF weighting (since ECF T_2>>ICF T_2). To obtain ECF-weighted results, the ECF/ICF T_2 values were reversed. To obtain equal ECF/ICF weighting, both ECF/ICF T_2 were set to 300*ms*. Water confined exclusively to ECF/ICF data was obtained with the original parameters (ICF weighted), but with water concentration for one compartment set to 100% while the other was set to 0%. Varying membrane/myelin permeability results were obtained with ICF weighted parameters, and the permeability ranged from 0 to 0.04 for the cuneatus image and 0 to 0.1 for the gracilis/RST images, where the ranges were chosen in comparison to ref[7]. The gracilis/RST input needed larger changes in p in order to see comparable FWHM differences as with the cuneatus input.

To test our technique, a simulation was run on an 8×8 array of circles (128×128, pixel size of $0.93\times0.93\mu m^2$), with water confined to within the circles. The expected q-space diffraction pattern (q×a=1.22, where a is the circle diameter) was obtained (data not shown).

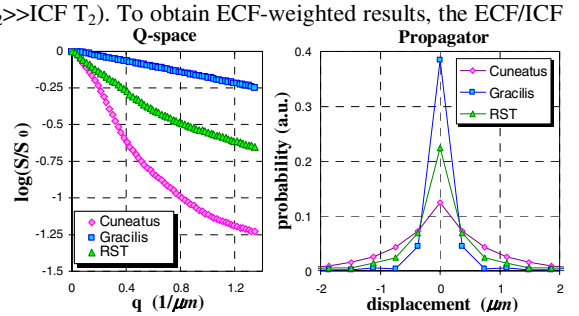

Fig. 2 Simulated q-space and propagator plots for cuneatus, gracilis, and RST input images with ICF-weighted parameters (zero permeability).

Table 1. FWHM values for various simulation parameters

Region	Histologic mean diameter	ICF weighted	ECF weighted	ICF/ECF equal	ICF only	ECF only	ICF weighted, variable permeability (p, $\mu m/ms$)	
Cuneatus FWHM (μm)	1.63 ± 1.02	1.01	1.06	1.03	1.00	1.16	1.20 (0.02)	1.27 (0.04)
Gracilis FWHM (μm)	0.90 ± 0.43	0.42	0.46	0.44	0.41	0.50	0.48 (0.04)	0.53 (0.1)
RST FWHM (μm)	1.09 ± 0.6	0.54	0.56	0.55	0.54	0.59	0.67 (0.04)	0.78 (0.1)

Results and Discussion

Fig. 2 shows simulated q-space and Pg plots with ICF weighted parameters (impermeable membrane). Table 1 lists the calculated Pg FWHM values for different simulation parameters and input images, with the exception of the first column, which lists the histology derived mean axon diameter and standard deviation. Unless otherwise noted, permeability was set to zero. All Pg FWHM values closely correlate with mean axon diameter. ECF/ICF weighting clearly has minimal effect of Pg FWHM. There is more difference when the water is restricted to only the ECF or ICF. Interestingly, the T_2 weighted (e^{-TE/T_2}) sum of ECF and ICF only FWHMs is similar to the ECF/ICF weighted FWHM values. As expected, increasing the permeability (p) broadens the propagator. However, the changes in FWHM were small relative to the wide range of permeability values.

Conclusion

Understanding the biophysical effects of ECF and ICF compartments on q-space behavior would aid in the interpretation of the method as applied to biological structures. Simulations on histologic images can therefore provide insight into the role of the various parameters. This preliminary work suggests that Pg FWHM values may be stable across a wide range of ECF/ICF T_2 and membrane/myelin permeability values. As the axons are closely packed, it can be seen from the histologic images that the size of ECF restrictions should be similar to that of ICF restrictions, and both should scale with axon size.

References: 1. Callaghan PT, *Principles of NMR Microscopy*, Oxford University Press (1991). 2. Assaf Y, *et al*, *MRM*, **44**:713-722 (2000) 3. Chin CL, *et al*, *MRM*, **52**:733-740 (2004). 4. Hwang SN, *et al*, *MRM*, **50**:373-382 (2003). 5. Stanisz GJ, *et al*, *MRM*, **37**:103-111 (1997). 6. Peled S, *et al*, *MRM*, **42**:911-918 (1999). 7. Disalvo EA, *Permeability and Stability of Lipid Bilayers*, CRC Press (1995). **Acknowledgements:** NIH grant R21 EB003951